SUPPORTING INFORMATION

Contents

S1. Experimental section

General procedures. Regular solvents were used for the synthesis of ruthenium complex **[Ru]** and the hybrid material **[Ru-rGO]**. In the catalytic experiments, alcohols and hydrosilanes were used as received from commercial suppliers. Anhydrous solvents were obtained using a solvent purification system (SPS M BRAUN) and used for the synthesis of the imidazolium salts.

Nuclear magnetic resonance (NMR) spectra were recorded on Varian spectrometers operating at 300 or 400 MHz (^{1}H NMR) and 75 or 100 MHz (^{13}C{^{1}H} NMR), respectively, and referenced to $SiMe_4$ (δ in ppm and J in Hertz). NMR spectra were recorded at room temperature with the appropriate deuterated solvent.

High-resolution images of transmission electron microscopy HRTEM and high-angle annular dark-field HAADF-STEM images of the samples were obtained using a Jem-2100 LaB6 (JEOL) transmission electron microscope coupled with an INCA Energy TEM 200 (Oxford) energy dispersive X-Ray spectrometer (EDX) operating at 200 kV. Samples were prepared by drying a droplet of a MeOH dispersion on a carbon-coated copper grid.

General procedure for the catalytic dehydrogenative coupling

Catalytic experiments were performed in a 25 mL round bottom flask, using 0.5 mmol of silane, 1 mL of alcohol, catalyst (0.05 – 1.00 mol %) and heating at 30 ºC under an initial aerobic atmosphere. The system was connected to an inverted burette filled with water that was used to collect the gas released and monitor de reaction. Yields and conversions were determined by GC analysis using anisole as internal standard. Isolated yields were determined by solvent evaporation and analysis by ^{1}H NMR spectroscopy using 1,3,5-trimethoxybenzene as external standard.

Large-scale catalytic experiment

Large-scale catalytic experiment was performed under the same conditions described in the general procedure. A 100 mL round bottom flask was charged with 68 mmol of silane (10 g) 50 mL of alcohol and 40 mg of **[Ru]** catalyst (0.068 mmol, 0.1 mol %). After completion of reaction (30 min), the solvent was removed by evaporation and the yield determined by gravimetric analysis.

Procedure for hydrogen identification

All glassware was carefully cleaned and rinsed with Milli-Q water prior to use. A 25 mL two-necked round bottom flask was charged with 1 mL of methanol and 6 mg (1 mol%) of **[Ru]** catalyst and stirred at room temperature for 5 min. Dimethylphenylsilane (1 mmol) was added with the aid of a syringe through a septum rubber. After 10 seconds, the gas evolved was captured with a syringe and injected in a quadrupole mass spectrometer equipment (Omnistar GSD 320 03 from PFEIFFER VACUUM) confirming the presence of molecular hydrogen.

S2. Reaction profile

The reaction between dimethylphenylsilane and methanol was monitored using a gas-burette setup (Figure S1). After the addition of the silane, the volume of gas evolved was recorded at different times (Figure S2).

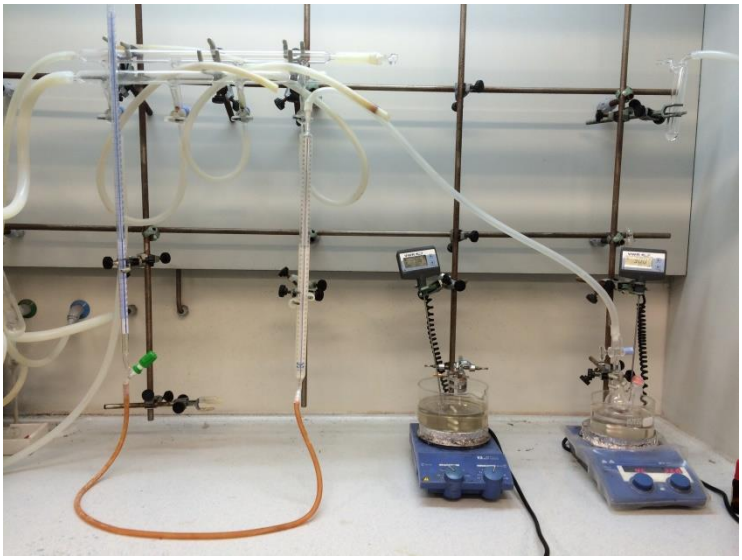

Figure S1. Experimental setup used for monitoring the dehydrogenative coupling reaction with an inverted burette.

S2.1 Reaction profile at different temperatures.

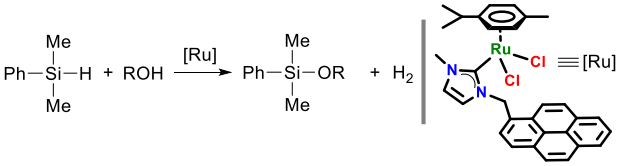

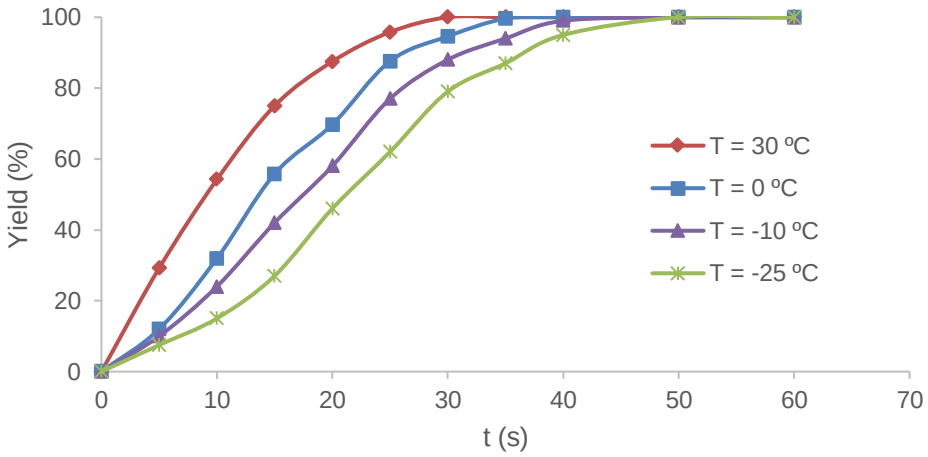

Figure S2. Reaction profile at different temperatures. Conditions: 1.0 mmol of dimethylphenylsilane, 1 mL of MeOH and 3 mg (0.5 mol %) of **[Ru]** catalyst. Yield corresponds to the amount of hydrogen collected using the system depicted in Figure S1.

S3. Nuclear Magnetic Resonance (NMR) Analysis

S3.1 ^{1}H NMR spectra of buthoxydimethylphenylsilane

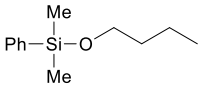

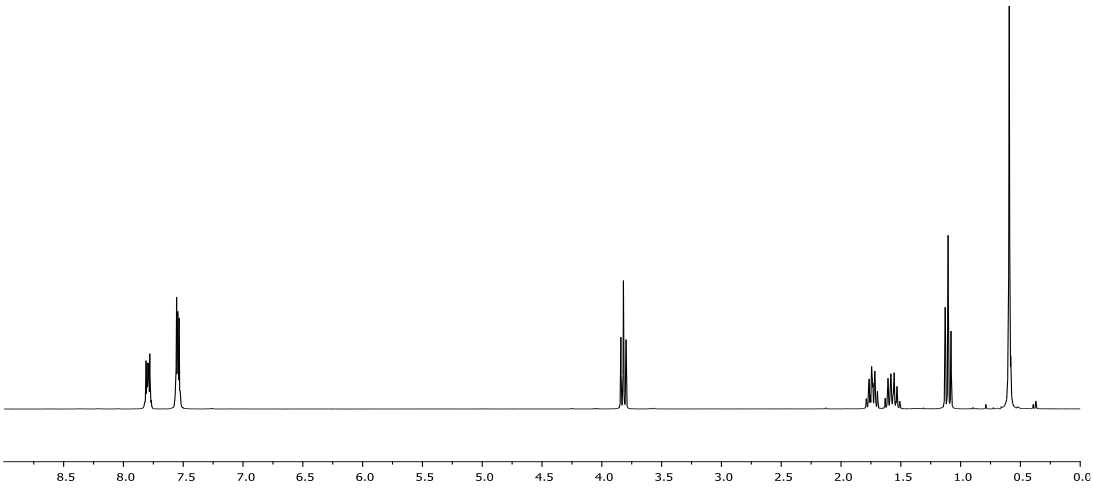

S3.2 ^{1}H NMR spectra of diethoxydiphenylsilane with 1,3,5-trimethoxybenzene used as reference

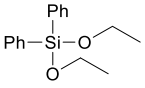

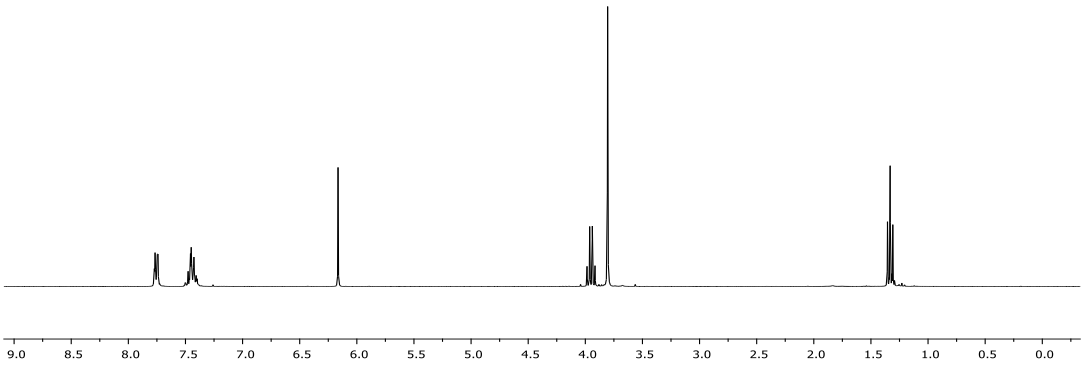

S4. Recycling experiments

S4.1 Recycling experiments using the material Ru-rGO

Recycling experiments were carried out under the reaction conditions used in the general procedure for the catalytic dehydrogenative coupling reaction. After completion of each run (10 min), the catalyst was isolated by decantation. The remaining solid was washed thoroughly with dichloromethane and alcohol and reused in the following run. We have not observed catalyst deactivation up to the tenth run.

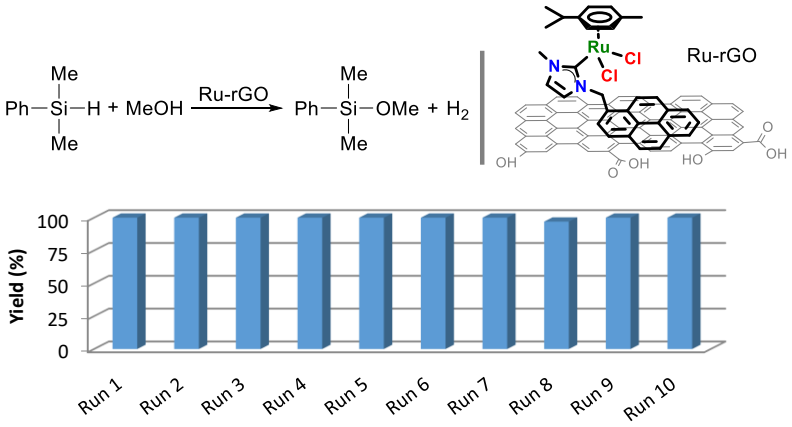

Figure S3. Reaction conditions: **Ru-rGO** supported catalyst 0.5 mol % Ru. In each run $Ph(Me)_2SiH$ (1.0 mmol) and 1 mL of MeOH were stirred for 10 min. Yields determined by GC using anisole as the standard.

S4.2 Stability of the ruthenium catalyst [Ru]: Sequential methanolysis of $PhMe_2SiH$

Methanol (1 mL) and **[Ru]** catalyst (1 mol %) were charged in a two-necked round bottom flask. One neck was connected to the experimental setup shown in Figure S1 and the other one was closed with a rubber septum. Using a syringe, $PhMe_2SiH$ (150µl, 1mmol) was added through the septum and the evolved gas was monitored. When the gas evolution was stopped, additional portions of silane were added. The results show that the molecular **[Ru]** catalyst is active after the addition of 6 portions of $PhMe_2SiH$ indicating the high stability of the complex. The time-profile shows that the reaction is slower after the addition of each portion of $PhMe_2SiH$ and the yield decreases to ca. 40%. Addition of methanol after the 6^{th} run, allows to boost the yield up to 95 %, revealing that consumption of methanol and generation of alkoxosilane in the media dramatically affects the kinetics of the reaction.

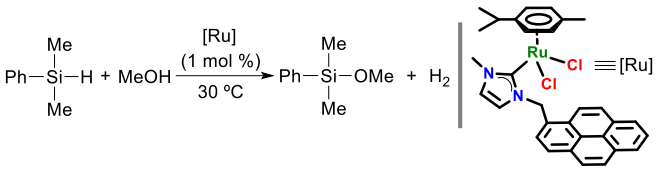

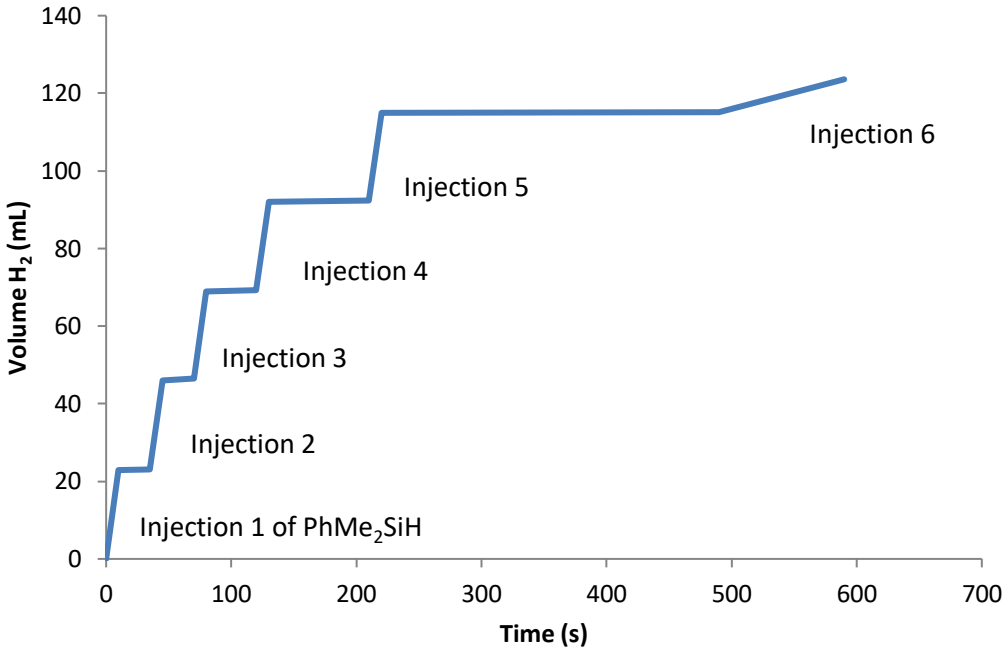

Figure S4. Time-profile for the reaction between dimethylphenylsilane and methanol obtained over six-additions of silane. An evolved volume of 24 mL corresponds to 100 % yield. From injections 1 to 4 quantitative yields were obtained. In the 5th injection the yield drops to 75% and in the last injection the yield decreases to 36 %.

S5. High Resolution Transmission Electron Microscopy (HRTEM) images

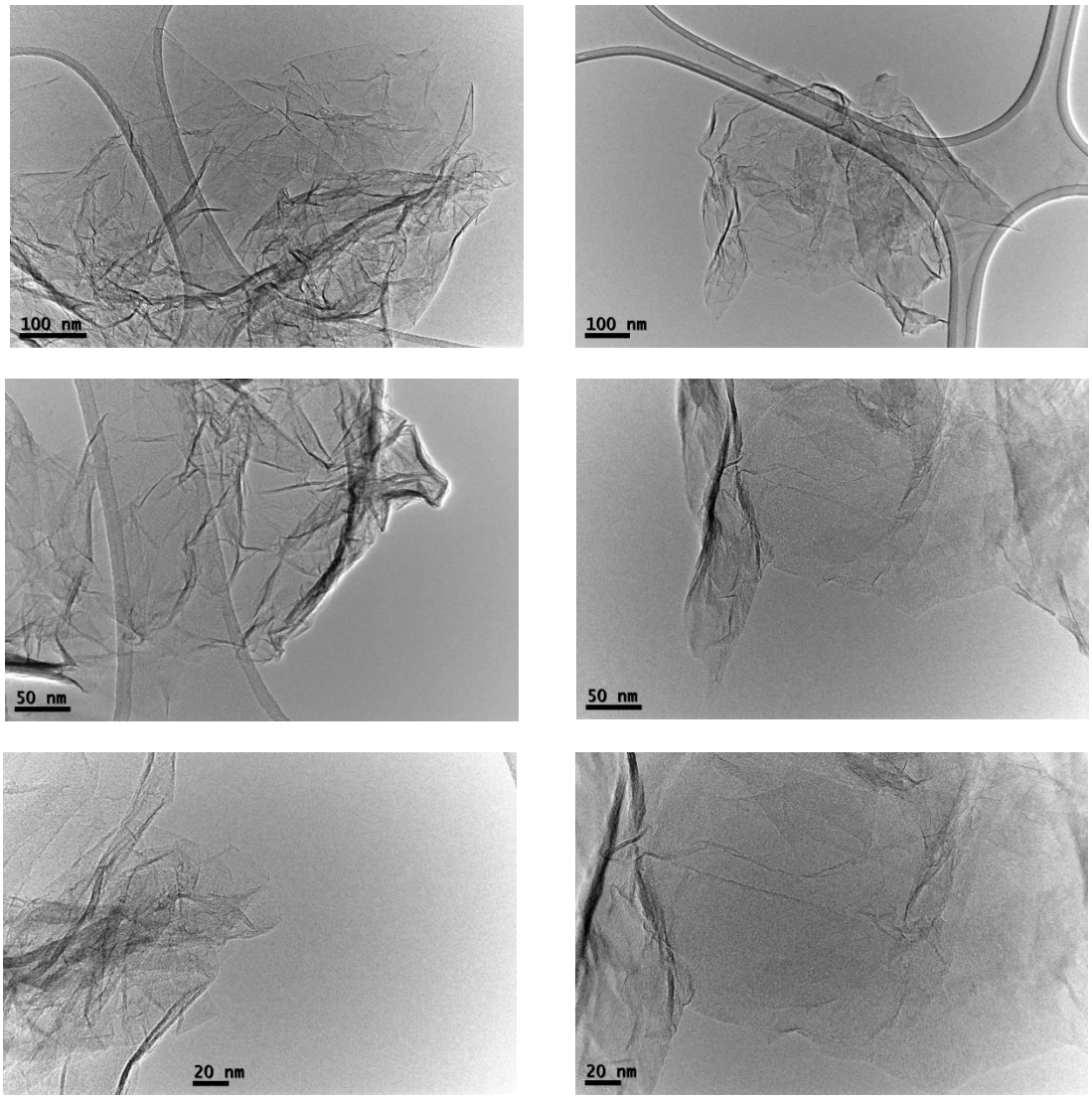

Figure S5. HRTEM images before (left) and after (right) ten catalytic cycles.

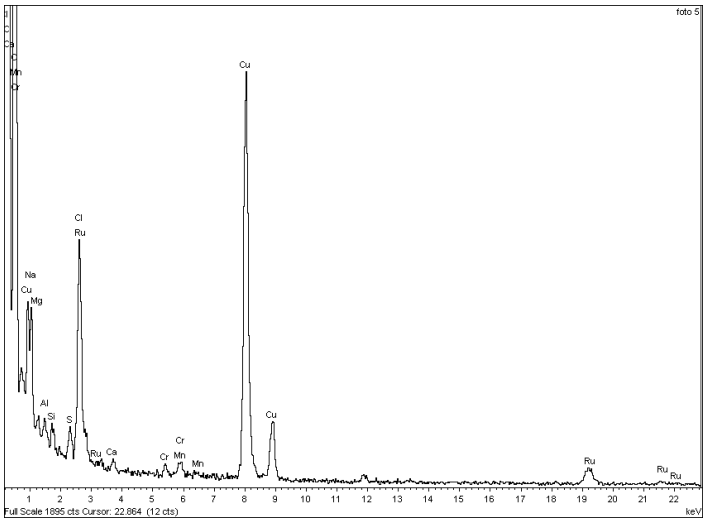

Figure S6. EDS spectrum of **[Ru-rGO]** after 10 catalytic cycles

S6. X-ray photoelectron spectroscopy (XPS)

X-ray photoelectron spectroscopy (XPS) spectra were acquired on a Kratos AXIS ultra DLD spectrometer with a monochromatic Al Kα X-ray source (1486.6 eV) using a pass energy of 20 eV. The photoelectron take off angle was 90^{o} with respect to the sample plane. To provide a precise energy calibration, the XPS binding energies were referenced to the C1s peak at 284.6 eV.

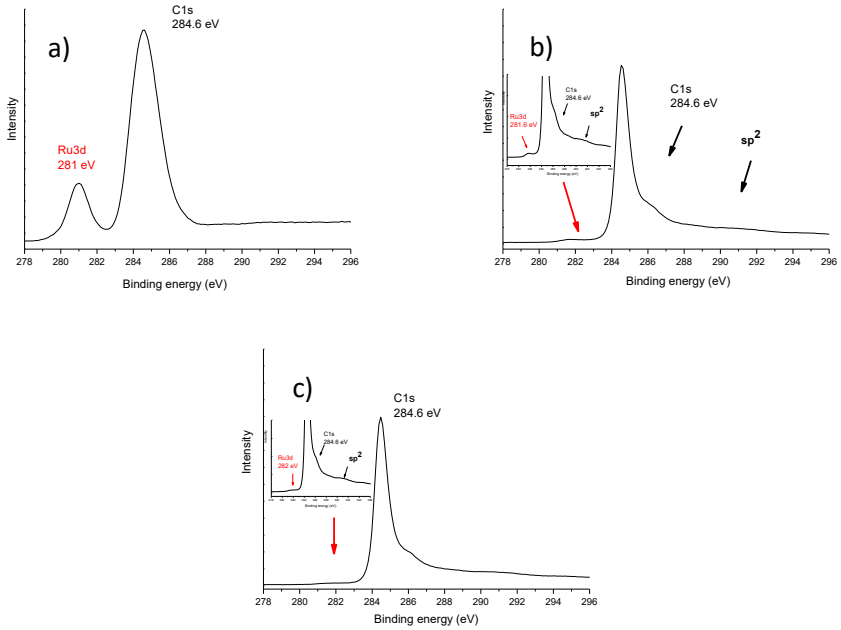

Figure S7. Ruthenium XPS spectra of **[Ru]** catalyst (a) and **Ru-rGO** catalyst before (b) and after (c) ten catalytic cycles.

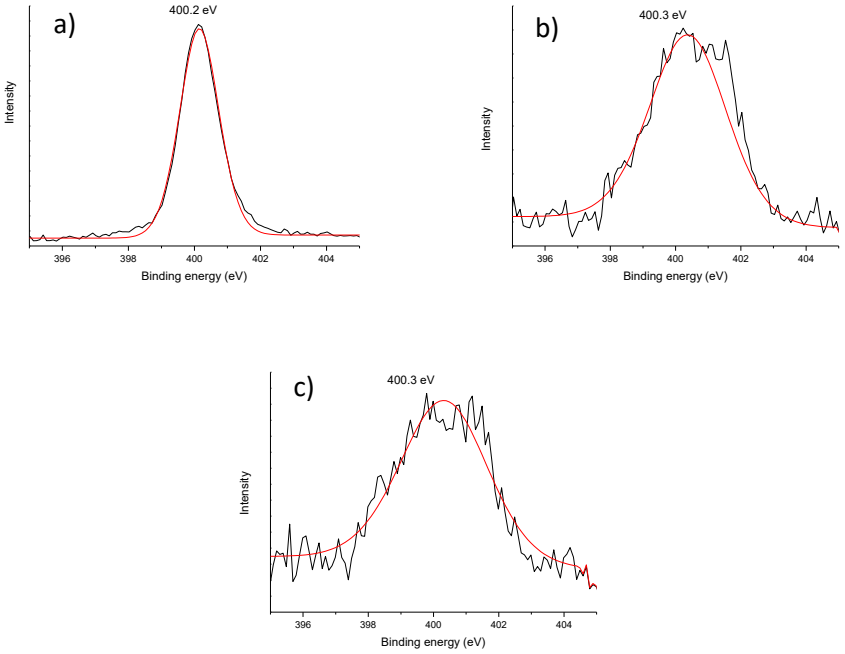

Figure S8. Nitrogen XPS spectra of **[Ru]** catalyst (a) and **Ru-rGO** catalyst before (b) and after (c) ten catalytic cycles.

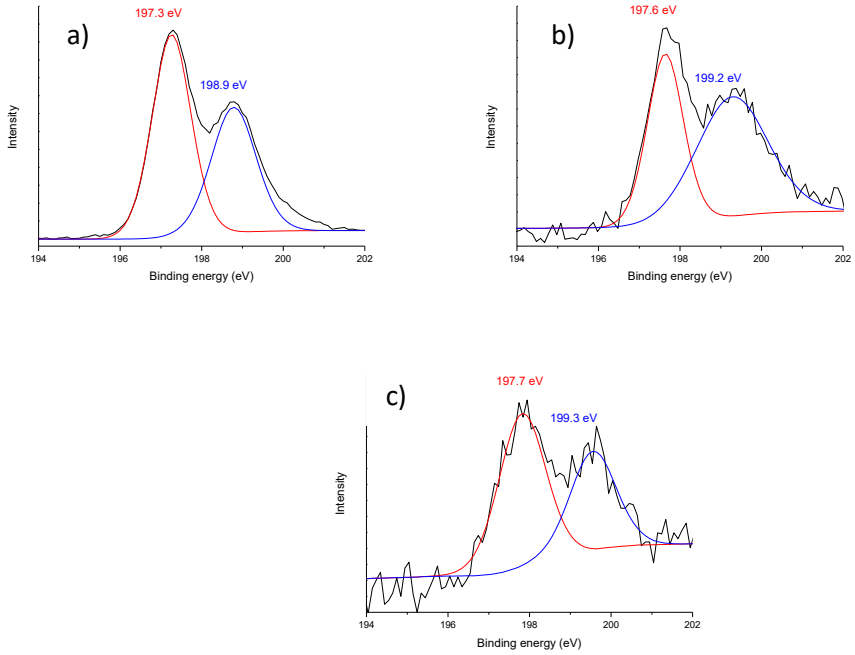

Figure S9. Chlorine XPS spectra of **[Ru]** catalyst (a) and **Ru-rGO** catalyst before (b) and after (c) ten catalytic cycles.

S7. DFT Calculations

S7.1 General comments

The dehydrogenative coupling of dimethylphenylsilane with methanol catalysed by a ruthenium complex has been studied by DFT calculations (Scheme S1). Details of theoretical methods and methodologies are in section 7.6. A selection of optimized geometries is included as an independent file, entitled *DFT-structures.xyz*.

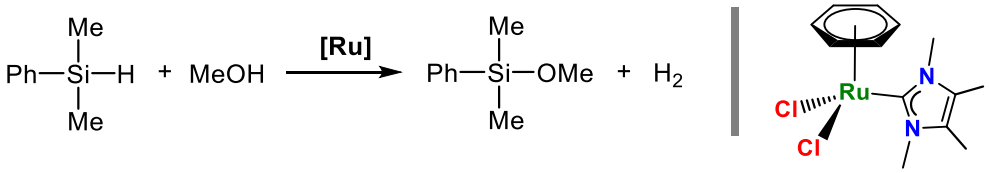

Scheme S1

Under the reaction conditions, dimethylphenylsilane, molecular hydrogen and methanol are present in the reaction media, along with the ruthenium catalyst. In order to gain insight onto the processes occurring in solution, the behaviour of the ruthenium starting material towards these reagents has been studied by DFT calculations.

S7.2 Behaviour of the ruthenium starting material towards dimethylphenylsilane.

The oxidative addition of the Si-H bond to the unsaturated $[Ru(\eta^6\text{-}C_6H_6)(NHC)(Cl)]^+$ metal fragment has been evaluated. Two minima have been located in the PES (Scheme S2.1). The most favoured geometry results from the interaction of the H-Si hydrogen of the silane with the metal centre, that is, via a η^1-H-SiR_3 interaction. No minima corresponding to an η^2-H-SiR_3 complex has been found. The second minima corresponds to a hydride silyl ruthenium (IV) derivative, but it is far less stable than the previous one ($\Delta G°$ = +21.2 kcal/mol). These results remark that the oxidative addition of silanes to the $[Ru(\eta^6\text{-}C_6H_6)(NHC)(Cl)_2]$ metal system is a disfavoured process.

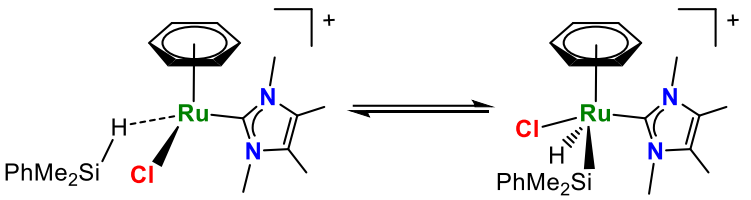

Scheme S2.1

The coordination of the silane σ bond to the unsaturated $[Ru(\eta^6\text{-}C_6H_6)(NHC)(Cl)]^+$ metal fragment has been further analysed by a freeze-scan strategy: starting from the Ru-η^1-H-SiR_3 minimum, the Si-Ru distance was shortened 0.1 Å, frozen, and the geometry was optimized by keeping this restriction. The procedure was repeated at different Si-Ru distances obtaining an energy profile (ΔE) for the Si-to-Ru approach (Scheme S2.2). The results suggest that the formation of a Ru-η^2-H-SiR_3 species is disfavoured with regard to the formation of a Ru-η^1-H-SiR_3, and that there is no evidence of a Ru-η^2-H-SiR_3 intermediate in the reaction profile.

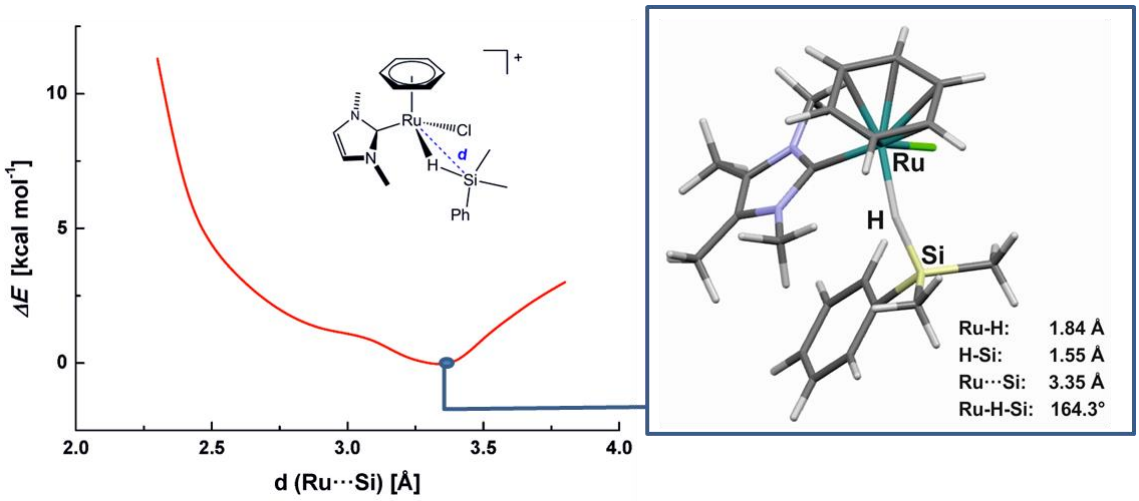

Scheme S2.2. Energy profile (ΔE) for the Si-to-Ru approach showing the geometry for the minimum.

S7.3 Behaviour of the ruthenium starting material towards molecular hydrogen.

The nature of the dihydride [Ru(η^6-C_6H_6)(NHC)ClH_2] complex has been studied by DFT calculations. Two minima have been located in the PES (Scheme S3). The most favoured structure is a dihydrogen ruthenium (II) complex. The second structure corresponds to a *transoid*-dihydride ruthenium (IV) species, which is clearly disfavoured (ΔG° = +15.3 kcal/mol).

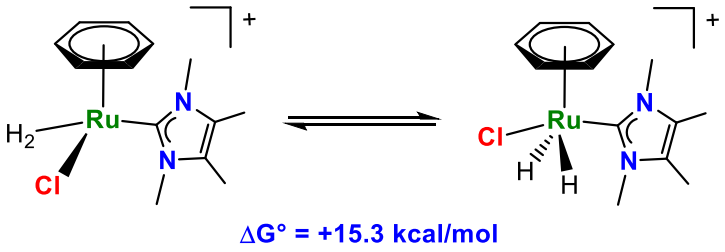

Scheme S3

S7.4 Equilibria between cationic solvento, η^1-silane and η^2-dihydrogen ruthenium systems.

Substitution of a chloride ligand from the starting material may produce three different species in solution: a solvento derivative resulting from methanol coordination, the η^1-silane adduct and a η^2-dihydrogen species (Scheme S4). The relative energies of the cationic derivatives have been evaluated by DFT calculations. The solvento derivative is the most favored species. The silane adduct is slightly disfavoured (ΔG° = +4.1 kcal/mol) and the dihydrogen derivative is much higher in energy (ΔG° = +8.8 kcal/mol).

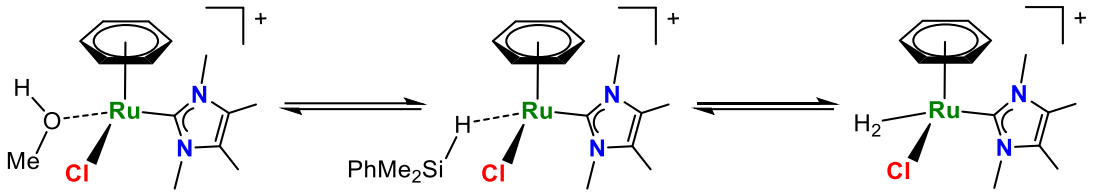

Scheme S4

S7.5 Mechanism proposal: Catalytic cycle and energy profile.

The behaviour of the ruthenium complex towards dimethylphenylsilane suggests that the catalytic process occurs via a $[Ru(\eta^6\text{-}C_6H_6)(NHC)(Cl)(\eta^1\text{-}H\text{-}SiMe_2Ph)]^+$ intermediate (**I**, Figure S10). The proposed mechanism involves the following steps: A) nucleophilic attack onto the silicon atom of the silane coordinated to ruthenium (**II**), leading to a neutral ruthenium hydride intermediate (**IV**); B) proton transfer from the resulting organic cation to the hydride complex (**V**), leading to a cationic ruthenium dihydride intermediate (**VI**); C) hydrogen evolution with concomitant silane coordination, therefore regenerating the cationic ruthenium silane intermediate (**VII**).

The complete free energy profile obtained by DFT calculations is fully consistent with experimental evidences. The reaction proceeds very fast at low temperatures (Figure S11). The rate limiting step is the methanol-assisted hydride transfer to the ruthenium centre (estimated $\Delta G^{\ddagger}$ = +8.0 kcal/mol). Subsequent proton transfer, hydrogen evolution and silane coordination are fast steps. Besides, hydrogen release is an irreversible process that keeps the catalytic reaction fast and quantitative.

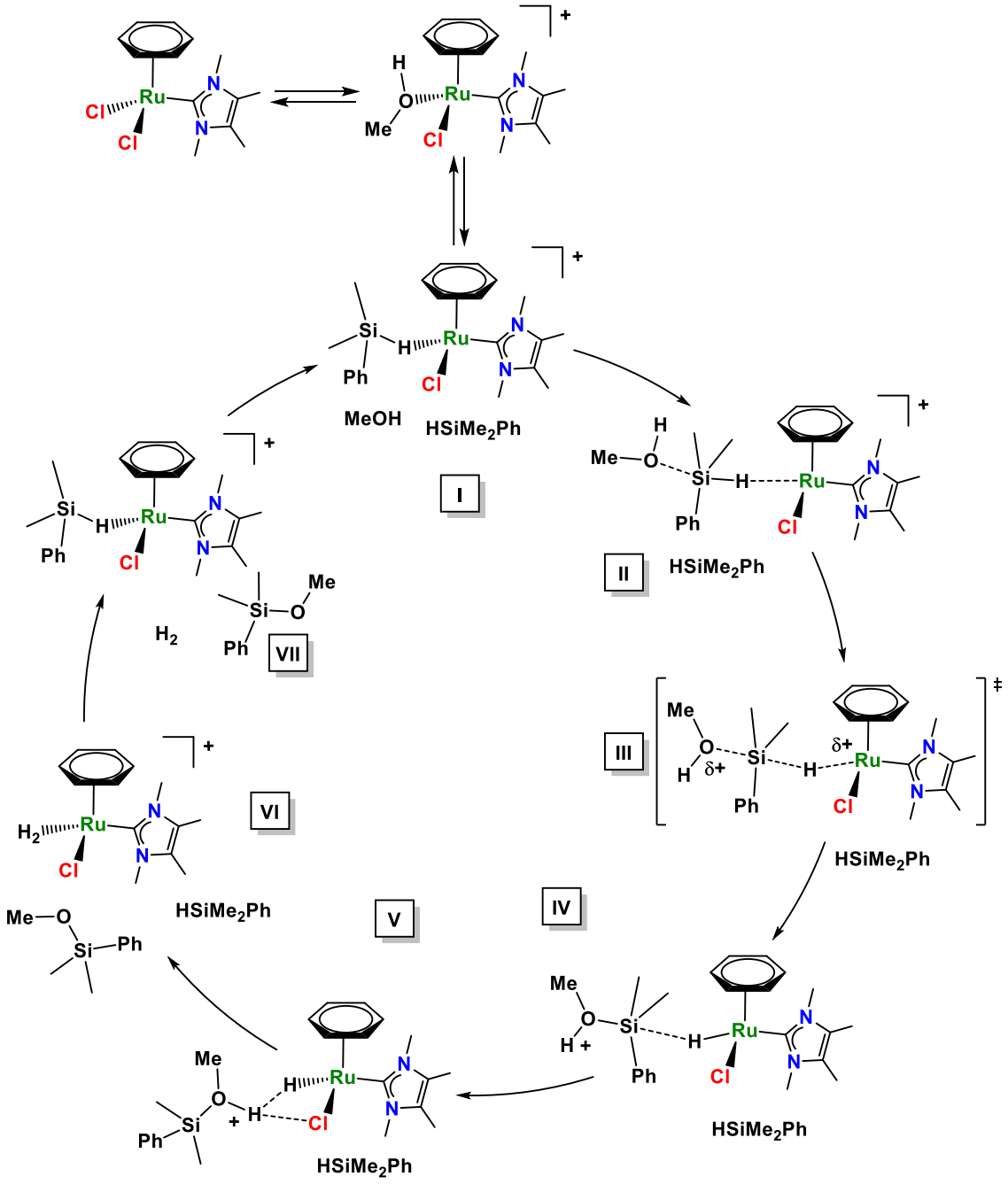

Figure S10. Mechanistic proposal for the dehydrogenative coupling of dimethylphenylsilane and methanol catalysed by [Ru(η^6-C_6H_6)Cl_2(NHC)].

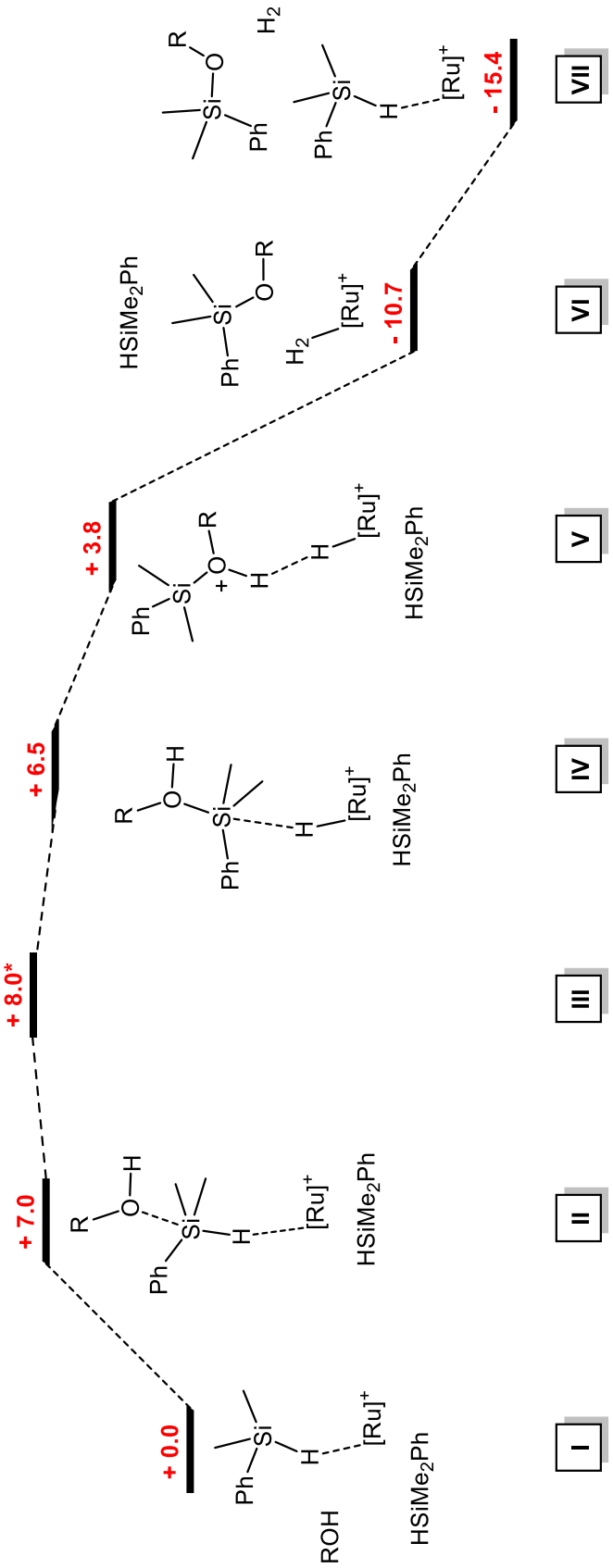

Figure S11. Complete free energy profile (kcal/mol) for the dehydrogenative coupling of dimethylphenylsilane and methanol catalysed by [Ru(η^6-C_6H_6)Cl_2(NHC)] in Kcal/mol.

S7.6 Mechanism proposal: Other considerations.

Consideration of other mechanism proposals implies the reactivity between Ru-arene complexes and silanes. In this regard, Ruthenium-arene complexes react with hydrosilanes to give ruthenium hydrides and silyl chlorides in completely dry solvents such as dichloromethane (Pathway A, Figure S12). However, such reactivity is not observed when using alcohols as solvent due to silylation of the polar solvent. Silyl chlorides (R_3Si-Cl) react with alcohols (such as MeOH) to yield silyl ethers (R_3Si-OMe) and hydrogen chloride. The latter immediately protonates the ruthenium-hydride complex giving rise to the corresponding cationic dihydrogen chloride derivative. This complex, which is present in our mechanism proposal, evolves molecular hydrogen and regenerates the unsaturated ruthenium complex that re-starts the catalytic cycle (Pathway B, Figure S12). Thus, our mechanistic proposal is analogous to pathway B but solvent-assisted (Pathway C, Figure S12). In all cases, the key-intermediates are the 16-VE ruthenium chloride species. Ruthenium-hydride species takes part in the cycle, but its half-life in acidic media is too short and therefore it is not observed experimentally. The instability of Si-Cl bonds in alcoholic media strongly supports the operation of pathway C over pathway B, as is shown in the catalytic cycle depicted in Figure S10.

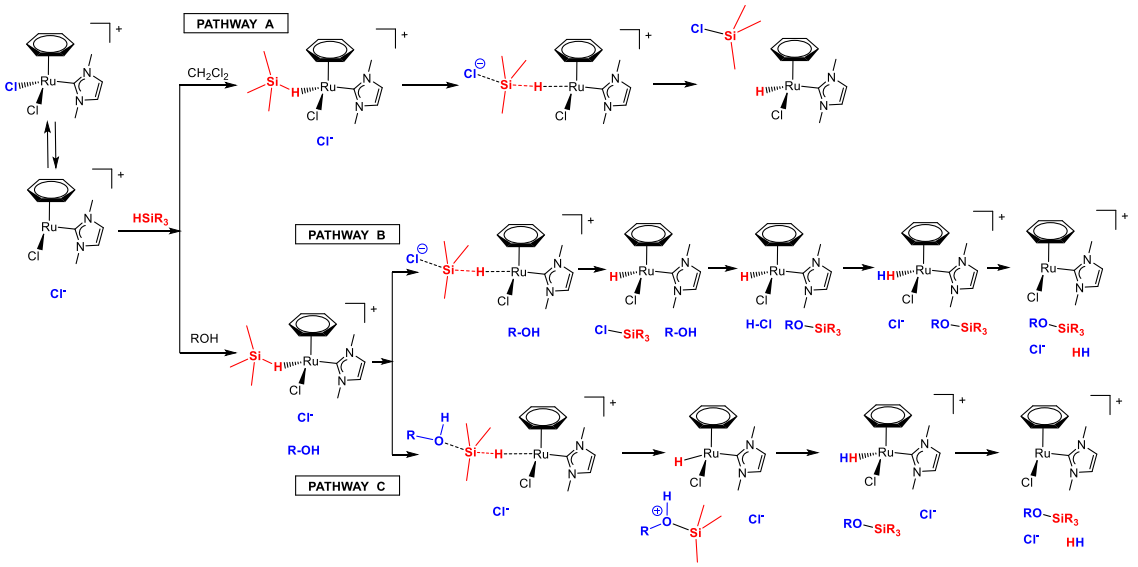

Figure S12. Mechanistic considerations in the reactivity between ruthenium complexes and hydrosilanes.

S7.7 Computational Details.

Quantum mechanical calculations were performed with the Gaussian09 package[S1] at the DFT/M06 level of theory.[S2] SDD basis set and its corresponding effective core potentials (ECPs) were used to describe the Ruthenium atom.[S3] An additional set of f-type functions was also added.[S4] Carbon, nitrogen, oxygen, silicon and hydrogen atoms were described with a 6-31G** basis set.[S5,S6] All calculations were performed in methanol solution (ε = 32.613) by means of the SMD continuum solvation model.[S7] The structures were freely optimized with no symmetry restrictions. Frequency calculations were subsequently performed in order to determine the nature of the stationary points found. No transition structures for the S_N2 processes could be

located, mainly because of the virtually barrierless nature of these processes. Instead they were carefully studied by using the following freeze-scan strategy: Si···O distances were frozen in subsequent 0.05 Å steps, and the structures were optimized with this geometrical restriction. Furthermore, this strategy was repeated by using 0.01 Å steps in the Si-O distance range from 2.00 to 1.85 Å, the critical range in which simultaneously the Si-O bond is forming, the Si-H bond is breaking and the H-H bond is forming. Such analysis afforded energy curves for the reaction coordinate connecting minima **II** and **IV** and an estimate of the transition state structure, with its corresponding electronic energy (E_{TS}*). The activation free energy was estimated by applying the expression $G^{‡}$* = $G_{(II)}$ + (E_{TS}* – $E_{(II)}$). A selection of DFT optimized geometries relevant for the discussion is included as an independent file entitled *DFT-structures.xyz*, which can be downloaded from the supplementary material.

S8. Catalyst resting state.

Determination of catalyst resting state was carried out using a 10 mol% catalyst loading under standard reaction conditions. In a 25 mL round bottom flask was dissolved (10 mg, 0.025 mmol) of [Ru(*p*-cym)$(Cl)_2$(Me_2-NHC)] in 1 mL of MeOH (Scheme S5). Addition of dimethylphenylsilane (39.1 µL, 0.25 mmol) at 30 °C shows a rapid bubbling. After no more gas evolution, the reaction mixture was stopped (< 5 min.). The volatiles were removed under reduced pressure and the residue was analysed by ^{1}H NMR using $CDCl_3$. The spectrum shows identical signals before and after the catalytic experiment indicating that the ruthenium [Ru(p-cym)$(Cl)_2$(Me_2-NHC)] species is recovered and corresponds to the catalyst resting state (Figure S13).

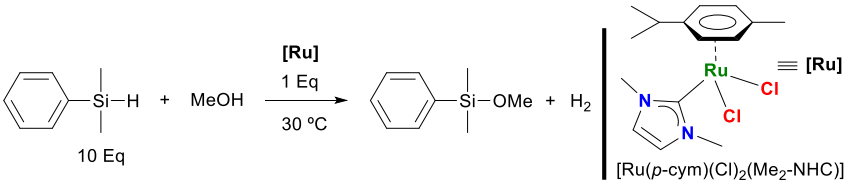

Scheme S5. Catalyst resting state determination

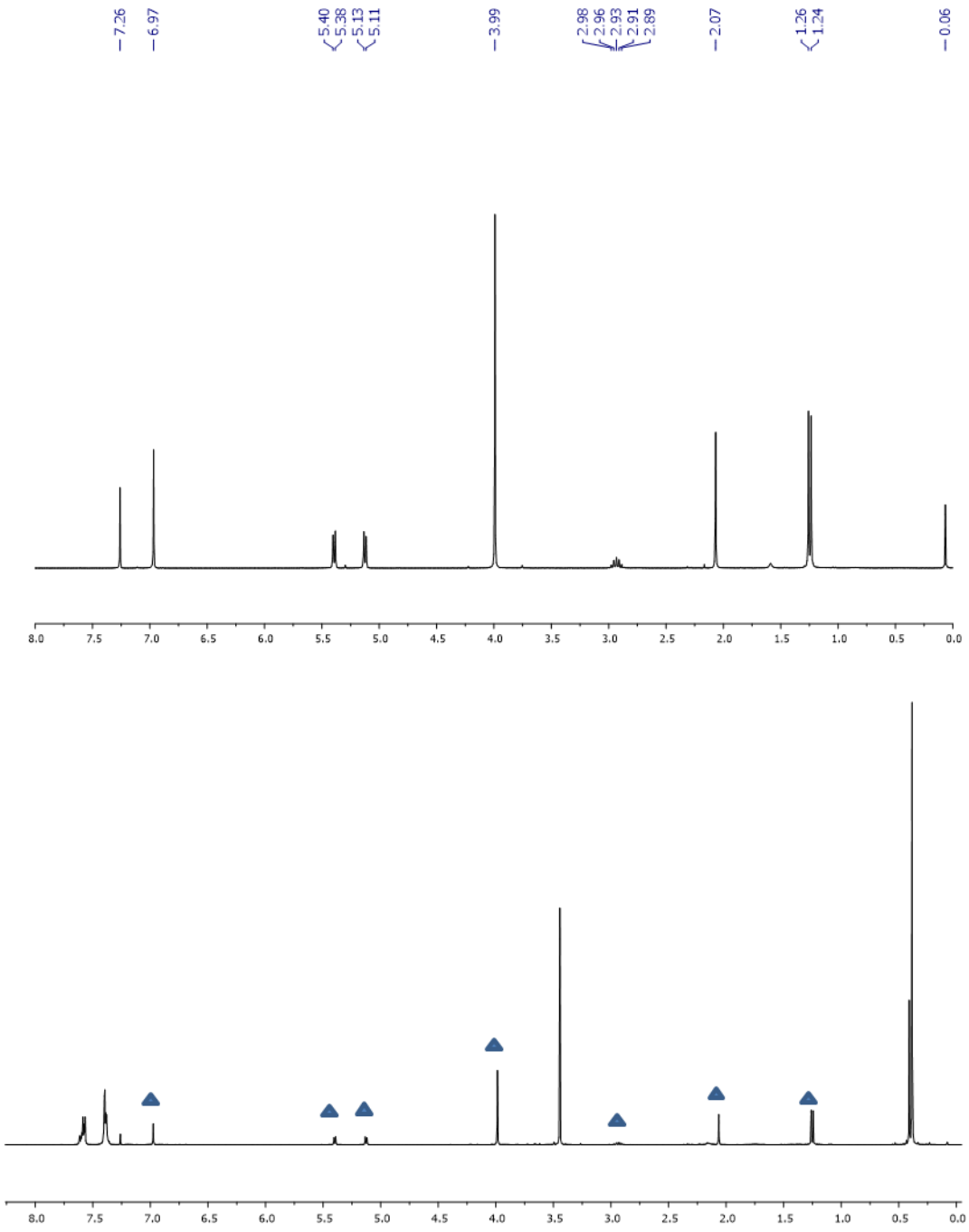

Figure S13. ^{1}H NMR of [Ru(*p*-cym)(Cl)$_2$(Me$_2$-NHC)] in $CDCl_3$ before (top) and after (down) the catalytic experiment. Signal marked with triangles correspond to the ruthenium catalyst and the rest of signals are the residual solvent $CDCl_3$ (7.2 ppm) and the silyl ether product $PhMe_2SiOMe$.

S9. References.

(S1) M. J. Frisch, G. W. Trucks, H. B. Schlegel, G. E. Scuseria, M. A. Robb, J. R. Cheeseman, G. Scalmani, V. Barone, B. Mennucci, G. A. Petersson, H. Nakatsuji, M. Caricato, X. Li, H. P. Hratchian, A. F. Izmaylov, J. Bloino, G. Zheng, J. L. Sonnenberg, M. Hada, M. Ehara, K. Toyota, R. Fukuda, J. Hasegawa, M. Ishida, T. Nakajima, Y. Honda, O. Kitao, H. Nakai, T. Vreven, J. A. Montgomery, Jr., J. E. Peralta, F. Ogliaro, M. Bearpark, J. J. Heyd, E. Brothers, K. N. Kudin, V. N. Staroverov, T. Keith, R. Kobayashi, J. Normand, K. Raghavachari, A. Rendell, J. C. Burant, S. S. Iyengar, J. Tomasi, M. Cossi, N. Rega, J. M. Millam, M. Klene, J. E. Knox, J. B. Cross, V. Bakken, C. Adamo, J. Jaramillo, R. Gomperts, R. E. Stratmann, O. Yazyev, A. J. Austin, R. Cammi, C. Pomelli, J. W. Ochterski, R. L. Martin, K. Morokuma, V. G. Zakrzewski, G. A. Voth, P. Salvador, J. J. Dannenberg, S. Dapprich, A. D. Daniels, O. Farkas, J. B. Foresman, J. V. Ortiz, J. Cioslowski, D. J. Fox; *Gaussian 09, Revision D.01* Gaussian, Inc., Wallingford CT, **2013**.

(S2) Y. Zhao; D. G. Truhlar; *Theor. Chem. Acc.* **2008**, *120*, 215-241.

(S3) D. Andrae; U. Häussermann; M. Dolg; H. Stoll; H. Preuss *Theor. Chim. Acta* **1990**, *77*, 123-141.

(S4) A. W. Ehlers; M. Böhme; S. Dapprich; A. Gobbi; A- Höllwarth; V. Jonas; K. F. Köhler; R. Stegmann; A. Veldkamp; G. Frenking *Chem. Phys. Lett.* **1993**, *208*, 111-114.

(S5) P. C. Harihara; J. A. Pople *Theor. Chim. Acta* **1973**, *28*, 213-222.

(S6) M. M. Francl; W. J. Pietro; W. J. Hehre; J. S. Binkley; M. S. Gordon; D. J. Defrees; J. A. Pople *J. Chem. Phys.* **1982**, *77*, 3654-3665.

(S7) A. V. Marenich; C. J. Cramer; D. G. Truhlar *J. Phys. Chem. B* **2009**, *113*, 6378-6396.